Journal of Controlled Release 390 (2026) 114577

Contents lists available at ScienceDirect

Journal of Controlled Release

journal homepage: www.elsevier.com/locate/jconrel

3D printed sex-specific medicines: Excipient-mediated modulation boosts systemic drug exposure by more than three-fold in male rats

Laxmi Prasanna Nandiraju [a], Patricija Januskaite [a], Siying Ruan [a], Yujia Qin [b], Iria Seoane-Viaño [a,c], Christine M. Madla [a,d], Keying Chen [b], Alvaro Goyanes [a,e,f,g,*], Yang Mai [b,*], Abdul W. Basit [a,e,*]

[a] UCL School of Pharmacy, University College London, 29-39 Brunswick Square, London WC1N 1AX, United Kingdom
[b] School of Pharmaceutical Sciences (Shenzen), Sun Yat-Sen University, Shenzen 518107, China
[c] Department of Pharmacology, Pharmacy and Pharmaceutical Technology, Paraquasil Group (GI-2109), Faculty of Pharmacy, iMATUS and Health Research Institute of Santiago de Compostela (IDIS), University of Santiago de Compostela (USC), Santiago de Compostela 15782, Spain
[d] UCL Business Ltd., 90 Tottenham Ct Rd, London W1T 4TJ, UK
[e] FABRX Ltd., Henwood House, Henwood, Ashford, Kent TN24 8DH, UK
[f] FABRX Artificial Intelligence, Calle Enrique Vidal Abascal 7 Bajo, Santiago de Compostela, CP 15702, Spain
[g] Departamento de Farmacología, Farmacia y Tecnología Farmacéutica, I+D Farma Group (GI-1645), Facultad de Farmacia, iMATUS and Health Research Institute of Santiago de Compostela (IDIS), Universidade de Santiago de Compostela (USC), Santiago de Compostela, 15782, Spain

ARTICLE INFO

Keywords:
Three dimensional printing of medicines
Printed oral drug delivery systems and drug products
Personalized formulations and dosage forms
Special populations
Sex differences in pharmacokinetics
Sex-specific personalisation of medications
Pharmaceutical excipients
Polyethylene glycol 2000

ABSTRACT

Excipients, historically regarded as inert, are now being recognised for their ability to actively modulate biological targets, including intestinal efflux transporters such as P-glycoprotein (P-gp). We have previously shown that polyethylene glycol (PEG) excipients can selectively enhance the oral bioavailability of P-gp substrate drugs, particularly in males. This study examined how 3D printed formulations containing PEG 2000 influence the pharmacokinetics of silodosin, a P-gp substrate drug used for the treatment of benign prostatic hyperplasia in ageing men, using male and female Wistar rats. Initial concentration screening studies with aqueous solutions revealed that a 1 % *w/v* PEG 2000 concentration (corresponding to 5 mg) maximally increased silodosin systemic exposure by 36 % compared to the control in males, with no significant effect in females, confirming sex-specific pharmacokinetic modulation. To exploit this unique phenomenon, 5 mg of PEG 2000 was incorporated as a functional excipient into silodosin-loaded printlets (3D printed tablets) fabricated *via* direct powder extrusion. The printlets achieved complete drug release within 70 min, exhibiting highly similar dissolution profiles between test and control formulations ($f_2 = 88.6$). *In vivo* pharmacokinetic studies revealed that printlets containing PEG 2000 resulted in a 213 % increase in plasma exposure in males relative to the control, while no significant enhancement was observed in females. By integrating biological variables such as sex into formulation design and leveraging the promising potential of 3D printing, this study demonstrates for the first time how excipient functionality can be harnessed to develop sex-specific oral therapies and advance personalised oral drug delivery. These findings pave the way for the future clinical translation of sex- and excipient-driven therapeutic approaches.

1. Introduction

Excipients, as defined by the US Food and Drug Administration (FDA) are “any component of a drug product other than an active ingredient” [1]. They constitute the majority of commonly prescribed oral formulations, accounting for approximately 71 % of their total mass [2]. Excipients were traditionally considered pharmacologically inert; however, growing evidence has revealed that they can actively modulate biological targets and alter drug pharmacokinetics (PK) [3–6]. Clinical studies have demonstrated that certain solubilising excipients, particularly polyethylene glycol (PEG) 400, can markedly enhance the oral bioavailability of P-glycoprotein (P-gp) substrate drugs such as ranitidine and cimetidine [7,8]. Interestingly, this enhancement was observed only in male but not female human subjects.

* Corresponding authors.
E-mail addresses: a.goyanes@fabrx.co.uk (A. Goyanes), maiy6@mail.sysu.edu.cn (Y. Mai), a.basit@ucl.ac.uk (A.W. Basit).

https://doi.org/10.1016/j.jconrel.2025.114577
Received 28 October 2025; Received in revised form 19 December 2025; Accepted 23 December 2025
Available online 25 December 2025

To further elucidate this phenomenon, a Wistar rat model was established, which successfully reflected the sex-specific effects observed in humans [9]. PEG 400 increased the oral absorption of P-gp substrate drugs, such as ranitidine and ampicillin in male rats, but showed no effect in females or on non-P-gp substrates like metformin [10]. This sex-dependent modulation is not unique to PEG 400 but extends to other polyoxyethylated excipients, including PEG 2000, Cremophor RH 40, Poloxamer 188, and Tween 80, all of which have substantially enhanced drug absorption in male rats [11]. P-gp expression levels in male and female Wistar rats also strongly correlate with those in humans [12], confirming their suitability as a preclinical model for studying sex differences in drug absorption mediated by P-gp. Collectively, these findings highlight the role of excipient-transporter interactions in influencing drug bioavailability and underscore the importance of considering sex as a biological variable in the design and evaluation of oral drug formulations.

Silodosin is a Biopharmaceutics Classification System (BCS) Class III drug and an α1-adrenergic antagonist indicated for benign prostatic hyperplasia (BPH), a urological condition that is highly prevalent in ageing men [13,14]. It exhibits an oral bioavailability of only 32 %, primarily due to limited intestinal permeability and active efflux mediated by P-gp transporters [15,16]. Therefore, leveraging the sex-specific effects of excipients could be especially advantageous for drugs with P-gp-limited absorption and for male-specific indications. Among the aforementioned excipients that elicit sex differences, PEG 2000 is particularly attractive for solid oral dosage forms because its waxy solid state allows ready incorporation into solid matrices, further supporting its suitability for oral drug delivery.

Emerging pharmaceutical manufacturing technologies, particularly three-dimensional printing (3DP), offer a versatile platform for integrating tailored excipient-drug systems into solid dosage forms [17–19]. Among the commonly used material extrusion-based methods, direct powder extrusion (DPE) has gained attention as a single-step process that merges the principles of hot-melt extrusion (HME) and fused deposition modelling (FDM) [20]. DPE offers several advantages, including eliminating filament preparation, fabricating dosage forms in varying sizes and geometries, accommodating high drug loads directly from powder blends, and enabling precise control over drug release kinetics [21–29]. In addition, DPE has been reported to be suitable for point-of-care applications in clinical settings, offering improved quality control capabilities [30,31]. While DPE has shown promise in facilitating the development of personalised medicines for a range of patient populations, including paediatric patients and individuals with chronic and rare diseases, this capability may also extend to the formulation of sex-optimised oral therapies, an area that remains largely unexplored [30–33].

We hypothesised that co-formulating silodosin with PEG 2000 would enhance its oral bioavailability. To study this, PK parameters of silodosin were evaluated following oral administration of both aqueous and solid formulations, with and without PEG 2000. Preliminary studies with aqueous solutions containing silodosin and varying concentrations of PEG 2000, along with a blank control, were conducted in Wistar rats. The PEG 2000 concentration that resulted in peak enhancement of silodosin absorption was selected for fabricating silodosin-loaded printlets (3D printed tablets), with (test) and without (control) PEG 2000, using DPE 3DP. Physicochemical characterisation was performed to determine printlet properties, including drug content and *in vitro* release profiles. This was followed by an *in vivo* PK study in male and female Wistar rats to investigate sex-related differences in silodosin absorption and systemic exposure.

2. Materials and methods

2.1. Materials

Eudragit® E PO (MW 150,000 g/mol) was obtained from Evonik Industries (Essen, Germany). PEG 2000 (MW 1800–2200 g/mol), talc (379.27 g/mol) and triethyl citrate (TEC, MW 276.28 g/mol, 99 %) were purchased from Sigma-Aldrich (Dorset, UK). Silodosin (MW 495.53 g/mol) was kindly gifted by Sun Pharmaceuticals Industries Limited (Gurugram, India). HPLC-grade water and acetonitrile (ACN, ≥99.9 % *v*/v, HPLC grade) were purchased from Fisher Scientific (Loughborough, UK). Potassium dihydrogen phosphate, disodium hydrogen phosphate, hydrochloric acid (5 M), and sodium hydroxide (1 N) were purchased from Thermo Fisher Scientific (Cheshire, UK).

2.2. Animals

All animal procedures were approved by the ethical review committee at Ruiye Model Animal (Guangzhou) Biotechnology Co. Ltd. in accordance with approval number RYEth-20230815298. Six male and six female Wistar rats (8 weeks old), each weighing approximately 200–250 g, were housed in the animal facility at Ruiye Model Animal (Guangzhou) Biotechnology Co. Ltd. under controlled conditions with room temperature maintained at 25 °C and a 12-h light and dark cycle. Rats were caged in groups of three, allowed to move freely, and provided with unrestricted access to food and water. All animals were acclimatised for a minimum of 7 days prior to the experiments. On the day before the study, rats were fasted overnight with free access to water for at least 12 h and housed individually in metabolic cages until the following morning.

2.3. Concentration-dependent effects of PEG 2000 on silodosin pharmacokinetics

2.3.1. Pharmacokinetic study of solution formulations

Aqueous solutions of silodosin co-formulated with varying concentrations of PEG 2000 were freshly prepared on the day of the experiment. Each solution was prepared to deliver a 12.5 mg dose of silodosin, corresponding to 50 mg/kg based on average rat weight, as established in previous studies [10], and PEG 2000 at concentrations of 0 % (control), 0.5 %, 1 %, 2 %, and 5 % *w/v*. Male and female Wistar rats ($n = 3$ per group) were administered 0.5 mL of the control or test solution by oral gavage. Blood samples (approximately 250–300 μL) were collected from the tail vein at predetermined time points: 10, 30, 60, 90, 120, 180, 240, and 360 min post-administration. At the end of the study, rats were euthanised in a CO_2 chamber (Schedule 1 method).

2.3.2. Liquid chromatography–tandem mass spectrometry (LC-MS/MS) analysis

Preparation of stock and working solutions: The stock solution was prepared by accurately weighing 10 mg of silodosin, moistening it with 10 μL of acetic acid, and dissolving it in 1 mL of water to obtain a 10 mg/mL solution. This stock solution was further diluted to prepare working solutions with concentrations of 200 ng/mL, 400 ng/mL, 1 μg/mL, 2 μg/mL, 4 μg/mL, 10 μg/mL and 20 μg/mL.

Preparation of calibration standards: Calibration standards in plasma were prepared by mixing equal volumes of blank rat plasma with each working solution at a 1:1 ratio, yielding final concentrations of 100 ng/mL to 10 μg/mL of silodosin. All calibration samples were freshly prepared on the day of the analysis.

Preparation of blood samples: All collected blood samples were centrifuged at 8000 rpm for 10 min at 4 °C to obtain plasma. For protein precipitation, methanol was added to each plasma sample at a ratio of 1:2 (plasma:methanol) and left for 10 min. The mixture was then vortexed thoroughly and centrifuged again at 8000 rpm for 10 min. The resulting supernatant was carefully collected and transferred into LC-MS/MS autosampler vials for analysis.

LC-MS/MS analysis: Quantification of silodosin in blood samples was performed using a Shimadzu LC-MS-8060 system (Shimadzu Co., Ltd., China) equipped with CBM-20A, LC-30AD, SIL-30AC, CTO-20AC, and MS-8060 modules. The validated LC method employed a mobile phase

consisting of 0.1 % formic acid in water (aqueous phase) and 0.1 % formic acid in ACN (organic phase). A gradient elution was applied, with the aqueous and organic phases run at 80:20 to 55:45 *v/v* from 0 to 6 min, followed by 80:20 *v/v* from 6 to 10 min. Chromatographic separation was achieved using an Acquity UPLC BEH C18 column (1.7 μm, 2.1 mm × 100 mm; Waters Limited, Wilmslow, UK) maintained at 40 °C. The flow rate was set at 0.4 mL/min, and the injection volume was 5 μL.

2.4. 3D printing

2.4.1. Pharma-ink preparation

The pharma-inks (drug-loaded ink) used for DPE were prepared by accurately weighing each component and manually blending the raw materials using a mortar and pestle. The compositions of the developed pharma-inks are presented in Table 1.

Each printlet was formulated to deliver a silodosin dose of 12.5 mg, equivalent to 50 mg/kg of rat body weight, as previously stated. Furthermore, 12.5 % *w/w* PEG 2000 corresponds to a mass of 5 mg per printlet, calculated based on the 1 % *w/v* concentration used in the solution PK study.

2.4.2. DPE 3D printing process

Size 9 capsule-shaped printlets, each measuring 8.60 mm in length and 2.65 mm in diameter, were fabricated using the M3DIMAKER™ pharmaceutical 3D printer (FABRX Ltd., London, UK) equipped with a direct single-screw powder extruder (DPE) and a 0.4 mm nozzle. The printlet geometry was designed using AutoCAD 2014 (Autodesk Inc., CA, USA), and the model was exported as a stereolithography (.stl) file to the printer software (Repetier-Host V2.1.3, Nordrhein-Westfalen, Germany) for processing. The prepared pharma-ink blends were loaded into the printer's hopper and manually guided into the nozzle using a spatula to maintain continuous flow during the printing process. The printing parameters applied for both test and control formulations are summarised in Table 2.

2.5. Printlet characterisation

2.5.1. Physical dimensions

The physical dimensions (length and diameter) of the printlets (n = 10) were measured using a digital calliper (Hilka Tools, Chessington, UK), and their individual masses were determined using an analytical balance.

2.5.2. Friability testing

Printlet friability was assessed using a Friability Tester Erweka type TAR 10 (Erweka GmbH, Heusenstamm, Germany). 20 printlets were randomly selected, weighed, and placed into the drum, which was rotated at 25 rpm for 4 min. The printlets were then reweighed, and friability was calculated as the percentage weight loss relative to the initial sample weight.

2.5.3. Thermal analysis

Thermogravimetric analysis (TGA) was performed to evaluate the thermal stability of the pure drug and individual excipients. Samples with an average mass of 3 mg were accurately weighed into open aluminium pans and heated from 30 °C to 400 °C at a rate of 10 °C/min using a Discovery TGA system (TA Instruments, Waters LLC, New Castle, DE, USA). Nitrogen was used as the purge gas at a flow rate of 25 mL/min. Data was collected and analysed using the TA instruments Trios software (v. 4.5.0.5), and the percentage mass loss *versus* temperature was calculated.

Table 1
Pharma-ink compositions for test and control formulations.

Pharma-ink	Eudragit® E PO (% *w/w*)	PEG 2000 (% *w/w*)	Silodosin (% *w/w*)	TEC (% *w/w*)	Talc (% *w/w*)
Test	38.25	12.50	31.25	8.00	10.00
Control	38.25	–	31.25	15.00	15.50

Table 2
Parameters applied during the 3DP process for both test and control printlets.

Printing parameter	Test printlets	Control printlets
Fill pattern	Rectilinear	Rectilinear
Infill (%)	100	100
Skirt and brim	No	No
Perimeter speed (mm/s)	10	10
Infill speed (mm/s)	5	5
Layer height (including first layer) (mm)	0.3	0.3
Extrusion temperature (°C)	85	80
Bed temperature (°C)	50	–

Differential scanning calorimetry (DSC) was used to characterise the thermal behaviour of silodosin, all individual excipients (excluding TEC), the pharma-inks, and printlets. DSC measurements were performed using a Q2000 DSC (TA instruments, Waters LLC, New Castle, DE, USA). An average of 3–5 mg of each sample was accurately weighed into Tzero aluminium pans, which were pinholed and sealed with hermetic Tzero lids (TA Instruments, Waters LLC, New Castle, DE, USA). Nitrogen was used as the purge gas at a flow rate of 50 mL/min. Calibration of the cell constant and enthalpy was performed using indium (Tm = 156.6 °C, ΔHf = 28.71 J/g) in accordance with the manufacturer's instructions. Samples were equilibrated at 23 °C, cooled to 0 °C at 10 °C/min, and then heated from 0 °C to 117 °C at the same heating rate. All data acquisition and analysis from the TGA and DSC experiments were performed using TA Instruments Universal Analysis 2000 software (version 4.5.0.5).

2.5.4. X-ray powder diffraction (XRPD) analysis

The XRPD patterns of pure powder samples (silodosin, Eudragit® E PO, talc and TEC), the pharma-inks, and printlets were obtained using a MiniFlex 600 X-ray diffractometer (Rigaku, Tokyo, Japan) equipped with a copper Kα X-ray source (λ = 1.5418 Å), with current and voltage set at 40 mA and 45 kV, respectively. The diffractograms were recorded over a 2θ angular range of 3–40°, with a step size of 0.02° and a scanning speed of 2°/min.

2.5.5. Fourier transform infrared (FT-IR) spectroscopy

FT-IR spectroscopy was conducted to assess the chemical compatibility of components within the control and test printlets. The spectra were collected using a Spectrum 100 FT-IR spectrometer (PerkinElmer, Waltham, MA, USA) over the range of 4000–650 cm^{-1} at a resolution of 8 cm^{-1} with 6 scans. Spectra were obtained for the pure drug (silodosin), all individual excipients, the pharma-inks, and the printlets.

2.5.6. Scanning electron microscopy (SEM) imaging

SEM imaging was performed to visualise the surface and cross-sectional morphology of the printlets. Printlets were cut in half and mounted onto a 25 mm aluminium stub using a self-adhesive carbon disc, followed by gold coating (25 nm) for 120 s using a sputter coater. The stub was then placed into a Quanta 200 FEG scanning electron microscope (Thermo Fisher Scientific, Loughborough, UK), operated at an accelerating voltage of 5–20 kV, with secondary electron detection used to capture the images.

2.5.7. Determination of drug content

Samples (n = 3) of both test and control printlets were individually placed in 100 mL volumetric flasks containing 100 % ACN and stirred magnetically until complete dissolution. The resulting solutions were filtered through 0.22 μm filters (Millipore Ltd., Dublin, Ireland), and the concentration of silodosin was determined using HPLC-UV.

2.5.8. High-performance liquid chromatography (HPLC) analysis

The assay was performed using a Hewlett Packard 1260 Series HPLC-UV system (Agilent Technologies, Cheadle, UK). Chromatographic separation was carried out on an Eclipse Plus C18 column (5 µm, 150 mm × 4.6 mm) (Agilent Technologies, Cheadle, UK) maintained at 25 °C. The mobile phase consisted of 25 mM potassium dihydrogen phosphate buffer (pH 7.0, adjusted with concentrated sodium hydroxide) and ACN in a 40:60 *v/v* ratio. The buffer solution was vacuum filtered prior to use. The flow rate was set at 1.0 mL/min, with an injection volume of 10 µL, and detection was performed at a wavelength of 269 nm.

The HPLC method was adopted directly from a previously published and validated method [34]. Prior to analysis, the stock solution was prepared by accurately weighing 10 mg of silodosin and dissolving it in 50 mL of ACN to obtain a concentration of 0.2 mg/mL. This stock solution was further diluted to prepare working standards, and a calibration curve was constructed over the concentration range of 2–200 µg/mL.

2.5.9. Disintegration study

Disintegration testing was performed using an Erweka ZT 34 disintegration testing apparatus (Erweka GmbH, Heusenstamm, Germany). Test and control printlets ($n = 3$ per group) were individually placed into the basket rack assembly and immersed in phosphate buffer adjusted to pH 3.9, maintained at 37 ± 0.5 °C. Disintegration was defined as the time point at which the eroded printlet escaped the mesh of the basket rack assembly, and the corresponding disintegration time was recorded.

2.5.10. In vitro drug release study

In vitro drug release profiles of the test and control printlets were evaluated using a USP-II mini paddle apparatus (Agilent Technologies, Stockport, UK). The printlets were placed in 100 mL of phosphate buffer adjusted to pH 3.9 using 5 M HCl for 2 h to simulate rat gastric conditions [35]. The paddle speed was set at 100 rpm, and the temperature of the dissolution medium was maintained at 37 ± 0.5 °C. 1 mL samples were manually withdrawn at predetermined time points and immediately replaced with an equal volume of fresh buffer. The collected samples were filtered through 0.22 µm filters (Millipore Ltd., Dublin, Ireland) and analysed using HPLC-UV to quantify the amount of silodosin released. All experiments were conducted in triplicate under sink conditions, and data were reported as mean ± standard deviation ($n = 3$).

2.5.11. f_2 similarity factor calculation

To compare the dissolution profiles of the test and control printlets, the similarity factor (f_2) was calculated. The f_2 metric quantifies the similarity between two drug release profiles and is defined by the following equation (Eq. 1):

$$f_2 = 50 \cdot \log\left\{\left[1 + \frac{1}{n}\sum_{t=1}^{n}(R_t - T_t)^2\right]^{-0.5} \cdot 100\right\} \quad (1)$$

where f_2 is the similarity factor, n refers to the number of observations, R_t is the average percentage of drug released from the reference (control) printlets, and T_t is the average percentage of drug released from the test printlets [36]. It was proposed that, for two dissolution profiles to be considered similar, a similarity factor of 50 or greater (*i.e.*, 50–100) should be attained [37].

2.6. Pharmacokinetic study of printlets

Male and female Wistar rats ($n = 6$, respectively) were administered a single dose of either the control or test printlet *via* oral gavage. As described previously, blood samples were collected from the tail vein at the following time points: 30, 60, 120, 180, 240, 360, and 480 min, and rats were euthanised in a CO_2 chamber (Schedule 1 method) at the end of the study. Blood samples were then prepared and analysed by LC-MS/MS as per the method described in 2.3.2.

Additionally, another PK study was conducted, in which male and female Wistar rats (n = 6, respectively) were administered silodosin solution alone (control) or silodosin solution containing 1 % *w/v* PEG 2000 (test).

2.7. Pharmacokinetic analysis

PK parameters (C_{max}, t_{max}, AUC_{0-360}, AUC_{0-480} and $AUC_{0-\infty}$) were calculated by non-compartmental analyses using Phoenix WinNonlin™ software version 8.5.2.4. (Certara, Pennsylvania, USA).

2.8. Statistical analysis

Two-way analysis of variance (ANOVA) was used to evaluate the statistical significance of differences between the obtained PK results. For results showing statistical significance, a *post hoc* Tukey test was performed to determine differences between individual groups of observations. A *p-value* of <0.05 was considered statistically significant. All analyses were conducted using GraphPad Prism version 10.4.1 (Massachusetts, USA).

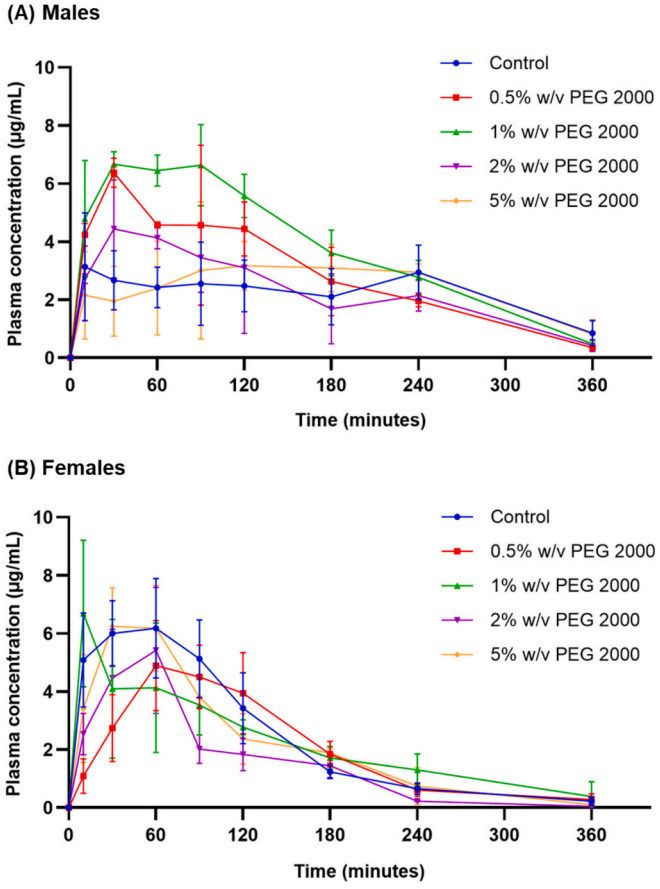

Fig. 1. *In vivo* mean plasma concentration–time curves of silodosin in the absence (control) and presence of PEG 2000 at 0.5 %, 1 %, 2 % and 5 % *w/v* concentrations in A) Male and B) Female Wistar rats. Data are presented as mean ± SD ($n = 3$).

3. Results and discussion

3.1. Concentration-dependent effects of PEG 2000 on silodosin oral absorption

The plasma concentration–time profiles and PK parameters of silodosin in male and female rats are represented in Fig. 1 and Table 3. In males, PEG 2000 produced distinct concentration-dependent profiles, with relatively flatter curves and longer T_{max} values (70–130 min at 1–5 % *w/v*) compared to the control (53 min). The highest C_{max} (7.02 μg/mL) and $AUC_{0-\infty}$ (1372.49 μg·min/mL) were observed at 1 % *w/v* PEG 2000, indicating enhanced systemic exposure at this concentration. At higher PEG 2000 concentrations, both C_{max} and $AUC_{0-\infty}$ appeared to decline. In females, however, the profiles displayed sharper, right-skewed peaks with more variable T_{max} values (10–80 min), while $AUC_{0-\infty}$ remained similar across all concentrations, with no clear concentration-dependent trend. Overall, PEG 2000 concentration appeared to influence silodosin plasma exposure, with the most notable enhancement observed at 1 % *w/v* in male rats.

The percentage difference in mean $AUC_{0-\infty}$ of silodosin against the control across varying PEG 2000 concentrations (0.5–5 % *w/v*) in male and female Wistar rats is shown in Fig. 2. The findings highlight a sex-specific modulation of silodosin drug absorption by PEG 2000. At 0.5 % *w/v*, both males (−10 %) and females (−14 %) showed a slight reduction in AUC compared to the control. The highest enhancement in silodosin exposure occurred at 1 % *w/v*, where males exhibited a significant increase of +36 % ($p<0.05$). In contrast, females at this concentration showed only a +3 % increase. At higher concentrations (2 % and 5 % *w/v*), silodosin plasma exposure declined again in both sexes, with reductions of −17 % and −2 % in males, and −35 % and −9 % in females, respectively. This can be attributed to a decreased intestinal transit time caused by the osmotic effects of PEG 2000, a known property of PEGs, which limits the absorption window in the small intestine and consequently reduces oral bioavailability [38,39].

The ability of PEGs to modulate P-gp function has been well documented across a range of molecular weights in *in vitro* intestinal permeability models, particularly using Caco-2 cell monolayers; however, studies examining their sex-dependent effects in animal models remain limited [40,41]. Silodosin is a known P-gp substrate, and the observed sex-specific increase in male rats may be linked to PEG 2000-mediated modulation of intestinal P-gp expression or activity, consistent with previous findings involving ranitidine [9]. Similarly, the absence of AUC enhancement in female rats also aligns with prior reports indicating that PEG 2000 does not influence P-gp function in females. Based on these findings, the 1 % *w/v* concentration of PEG 2000, which produced the peak percentage increase in AUC in male rats, was selected for co-formulation with silodosin in the 3D printlets for subsequent studies.

Table 3
Influence of PEG 2000 concentration on the PK parameters of silodosin in male and female Wistar rats. Data are presented as mean ± SD ($n = 3$).

Concentration of PEG 2000 (% *w/v*)	Sex	T_{max} (min)	C_{max} (μg/mL)	AUC_{0-360} (μg.min/mL)	$AUC_{0-\infty}$ (μg.min/mL)
Control	Male	53.33 ± 40.42	4.14 ± 1.06	781.93 ± 140.24	1052.87 ± 244.09
	Female	60.00 ± 30.00	6.55 ± 1.43	844.18 ± 183.13	871.52 ± 178.60
0.5	Male	20.00 ± 17.32	4.25 ± 3.70	1010.60 ± 149.87	1041.05 ± 146.84
	Female	80.00 ± 17.32	5.60 ± 1.04	699.91 ± 47.30	728.05 ± 61.08
1	Male	70.00 ± 34.64	7.02 ± 0.76	1327.89 ± 52.93	1372.49 ± 71.89
	Female	10.00 ± 0.00	6.69 ± 2.52	775.76 ± 110.78	855.87 ± 183.71
2	Male	70.00 ± 45.83	5.50 ± 0.91	804.07 ± 219.36	857.94 ± 234.57
	Female	50.00 ± 17.32	5.63 ± 1.88	540.48 ± 62.34	543.43 ± 62.77
5	Male	130.00 ± 45.83	4.43 ± 0.70	849.92 ± 150.62	1155.09 ± 108.06
	Female	50.00 ± 17.32	7.09 ± 0.14	768.49 ± 47.05	776.14 ± 51.00

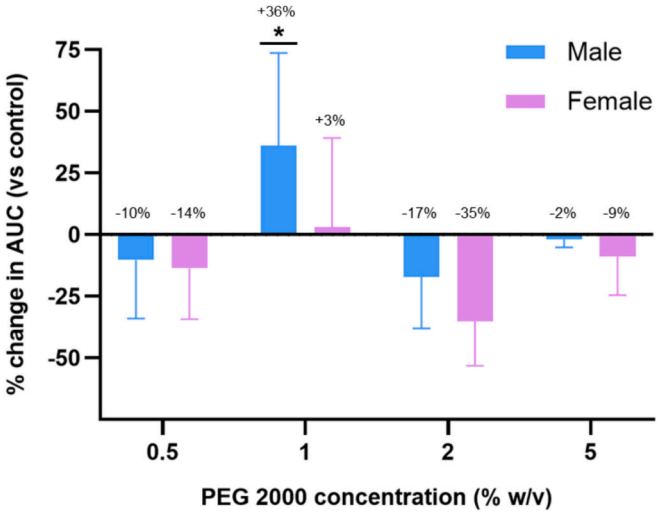

Fig. 2. Percentage change in the mean plasma $AUC_{0-\infty}$ of silodosin in male and female Wistar rats relative to the control and across different PEG 2000 concentrations: 0.5 %, 1 %, 2 %, and 5 % *w/v*. Data are presented as mean ± SD ($n = 3$). Statistically significant differences are indicated as follows: $p<0.033$ (*), $p<0.002$ (**), $p<0.001$ (***).

3.2. DPE 3D printing

A typical pharma-ink for extrusion-based 3DP such as DPE consists of a model drug and excipients including a polymer matrix, plasticisers, bulking agents, and lubricants to support printability. In this study, excipient selection was guided by both functional properties and the objective of accurately assessing the effect of PEG 2000 on silodosin absorption. Excipients which were known to influence intestinal permeability or interact with P-gp were excluded. For example, mannitol and magnesium stearate, commonly used as a bulking agent and a lubricant, respectively, were not included. Mannitol is a well-established paracellular transport marker [42], while magnesium stearate contains stearic acid derivatives that have been reported to interact with P-gp [43,44].

PEGs of various molecular weights are widely used as plasticisers in 3DP [45–47]. PEG 2000, in addition to being the excipient of interest in this study, also served as a plasticiser in the formulation. Other plasticisers commonly used in extrusion-based 3DP, such as citric acid monohydrate and triethyl citrate (TEC), were also considered [48,49]. However, citric acid monohydrate has been reported to downregulate P-gp and increase the oral absorption of P-gp substrates such as astilbin [50], and was therefore excluded. To our knowledge, no studies have indicated that TEC affects P-gp.

Silodosin has a low melting point of 105–109 °C, requiring the pharma-ink to be optimised at lower printing temperatures to maintain drug stability [15]. Eudragit® E PO, an immediate-release polymer with a low glass transition temperature (T_g) of 52.1 °C [51], was selected as the polymer matrix. However, as it melts quickly above its T_g, talc was added as a non-melting filler to improve the mechanical strength of the extrudate and enhance printability. TEC was also included as an additional plasticiser, allowing further reduction of the printing temperature. Its liquid nature also aided in binding the dry powders together and facilitated smooth feeding of the pharma-ink into the printer feeder. Based on the literature available at the time of formulation

development, neither Eudragit® E PO nor talc were reported to interact with intestinal P-gp.

Size 9 capsule-shaped printlets containing silodosin, without (control) and with (test) PEG 2000, were successfully printed using DPE, as shown in Fig. 3A and B, respectively. Despite the small size, uniform layer-by-layer printing was achieved, demonstrating the robustness of the DPE process.

Both printlet formulations showed consistent dimensions, with only slight deviations from the theoretical values (8.60 mm in length and 2.65 mm in diameter), with the length being more variable than the diameter (Table 4). Despite this, good uniformity in weight was observed, with all printlets weighing approximately 40 mg. Drug content studies showed that both formulations contained nearly 100 % of the expected 12.5 mg of drug per printlet, confirming that no drug loss occurred during the printing process. The friability values of the control and test printlets were 0.19 % and 0.48 %, respectively, which are within the acceptable pharmacopeial limit (< 1.0 %, USP), confirming adequate mechanical robustness for handling and packaging [52].

3.3. Characterisation of the DPE printlets

3.3.1. Thermal, XRPD and FT-IR analyses

TGA analysis was conducted to ensure that no degradation occurred at or below the selected printing temperatures. TGA thermograms (Fig. 4) confirmed that the drug and excipients remained stable at the printing temperatures of 80 °C (control) and 85 °C (test). Degradation of Eudragit® E PO, PEG 2000, and silodosin was initiated at temperatures above 250 °C, while talc showed negligible weight change across the tested temperature range. In contrast, TEC displayed thermal degradation just above 100 °C, which was a key factor in setting the maximum allowable printing temperature during formulation development. Accordingly, excipient selection and their proportions were optimised to enable printing at low temperatures, while maintaining suitable mechanical strength and dissolution performance in the final printlets.

DSC and XRPD analyses were carried out to evaluate the thermal behaviour and solid-state properties of the individual formulation components and investigate any physical changes occurring as a result of the 3DP process. As shown in Fig. 5, Eudragit® E PO exhibited a T_g of 56 °C, while PEG 2000 presented a broad endothermic peak around 45 °C, indicative of its melting behaviour. Silodosin showed a sharp endothermic peak at 103 °C, characteristic of its crystalline nature. In contrast, talc displayed no significant thermal events, confirming its high thermal stability. TEC was excluded from DSC analysis due to its liquid state and known thermal degradation above 100 °C, as seen in the TGA thermogram (Fig. 4). The DSC thermograms of the control pharma-ink and printlets revealed a distinct melting peak for silodosin, with a significant melting point shift to a lower temperature, suggesting partial interaction with the excipient matrix. In comparison, the test pharma-ink and printlets exhibited only minor baseline transitions, indicating possible solubilisation of silodosin within the excipient mixture facilitated by PEG 2000.

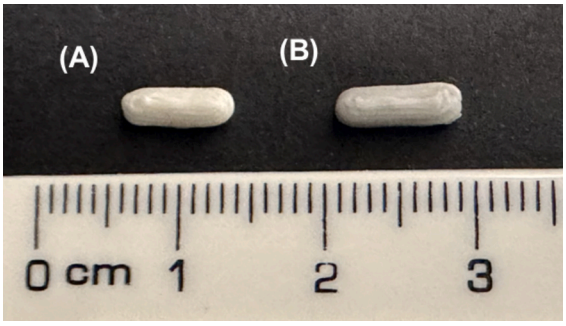

Fig. 3. Image of the printlets (A) control, and (B) test.

Table 4
Summary of dimensions (n = 10), weight (n = 10), drug content (n = 3) and friability of control and test printlets. Values are presented as mean ± SD, except for friability.

Formulation	Length (mm)	Diameter (mm)	Weight (mg)	Drug content (%)	Friability (%)
Control	7.86 ± 0.23	2.66 ± 0.04	40.58 ± 1.04	104.04 ± 4.64	0.19
Test	8.09 ± 0.24	2.71 ± 0.08	40.45 ± 0.67	99.27 ± 1.71	0.48

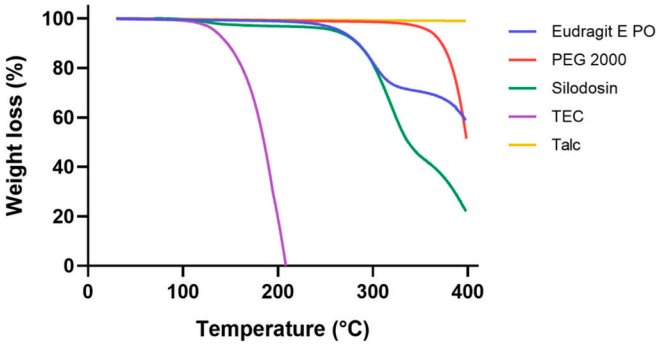

Fig. 4. TGA thermograms of pure silodosin and excipients.

These findings are supported by XRPD diffractograms (Fig. 6), where sharp peaks were observed for pure silodosin, but became attenuated in both control and test printlets after printing. Notably, the absence of silodosin's distinctive peak at 9° further indicates partial amorphisation during the DPE printing process. Additionally, the XRPD diffractogram of PEG 2000 showed broad peaks at approximately 18° and 22°, which, along with its broad DSC melting peak, suggest a semi-crystalline nature composed of both amorphous and crystalline regions.

FT-IR spectroscopy was performed to assess the chemical compatibility of silodosin and the excipients within the pharma-inks and printlets. As shown in Fig. 7, the FT-IR spectrum of silodosin exhibited characteristic bands, including a broad N—H/O—H stretching band in the 3400–3200 cm^{-1} region, aliphatic C—H stretching vibrations between 3000 and 2850 cm^{-1}, and multiple C═O and aromatic C═C stretching bands in the 1700–1500 cm^{-1} region [53]. Similarly, Eudragit® E PO exhibited aliphatic C—H stretching at 2950–2850 cm^{-1} and a characteristic ester C═O stretching band near 1730 cm^{-1}. PEG 2000 showed a broad O—H stretching band at 3450–3200 cm^{-1} and strong ether C—O—C stretching at 1150–1050 cm^{-1}, while TEC displayed a prominent ester C═O stretching band near 1735 cm^{-1}. Talc showed characteristic Si—O/Mg—O lattice vibrations below 1100 cm^{-1}, consistent with its inorganic nature [54].

The spectra of the pharma-inks and the printlets showed superposition of the individual component bands, particularly in the 1800–700 cm^{-1} region, confirming successful incorporation of silodosin and other excipients into the polymer matrix. Additionally, the spectra showed retention of all characteristic absorption bands of silodosin and the excipients in both control and test printlets, with no appearance of new peaks or significant peak shifts following printing. The slight broadening of certain drug and excipient peaks in the pharma-inks and the printlets is likely a result of the partial solubilisation of silodosin within the polymer matrix, as also observed in the DSC and XRPD analyses. Collectively, these findings indicate the absence of chemical degradation or drug-excipient incompatibility during the DPE 3D printing process.

3.3.2. SEM imaging

SEM images were obtained to investigate the surface and cross-

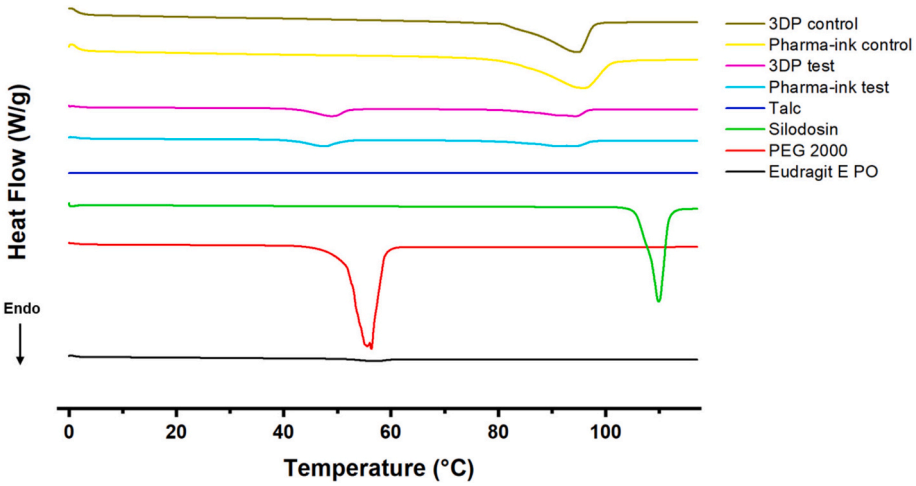

Fig. 5. DSC thermograms of pure silodosin, excipients, pharma-inks and the printlets.

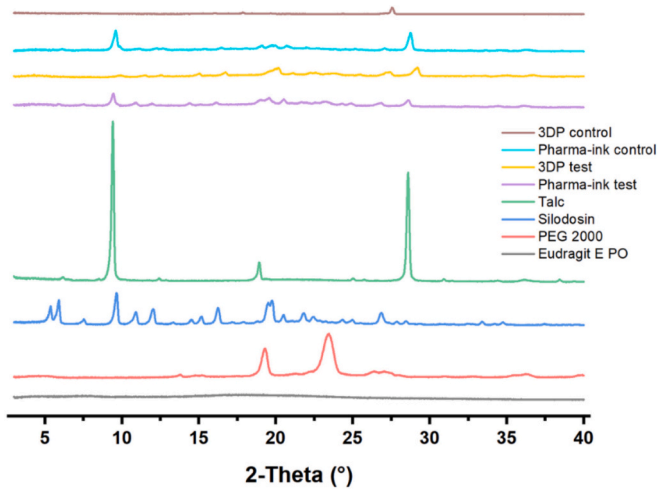

Fig. 6. X-ray powder diffractograms of pure silodosin, excipients, pharma-inks and the printlets.

sectional morphology of the printlets. As shown in Figs. 8A and C, the printed layers of both the control and test printlets appear uniform and tightly bound. The cross-section of the test printlet (Fig. 8D) is smooth, with more clearly defined layers, whereas the control printlet (Fig. 8B) displays a rougher surface and cross-section. This difference may be attributed to the absence of PEG 2000 in the control formulation. These observations suggest that PEG 2000 exhibits effective plasticising properties and contributes to improved structural integrity in the printlets.

3.3.3. *In vitro disintegration and drug release*

The disintegration times of the control and test printlets were 33.1 ± 8.4 min and 37.5 ± 1.8 min, respectively. The printlets did not fragment but uniformly reduced in size over time. This is consistent with the disintegration behaviour exhibited by formulations produced by material extrusion-based 3D printing [30,55]. Instead of fragmenting, the polymer-based matrix undergoes gradual surface erosion, causing progressive reduction in printlet dimensions over time.

The release profiles of silodosin from the control and test printlets are shown in Fig. 9. Dissolution testing was conducted in phosphate buffer at pH 3.9 to simulate the gastric environment of rats [35]. The gastric emptying time in rats typically ranges from 0.7 to 2 h [56,57]; therefore,

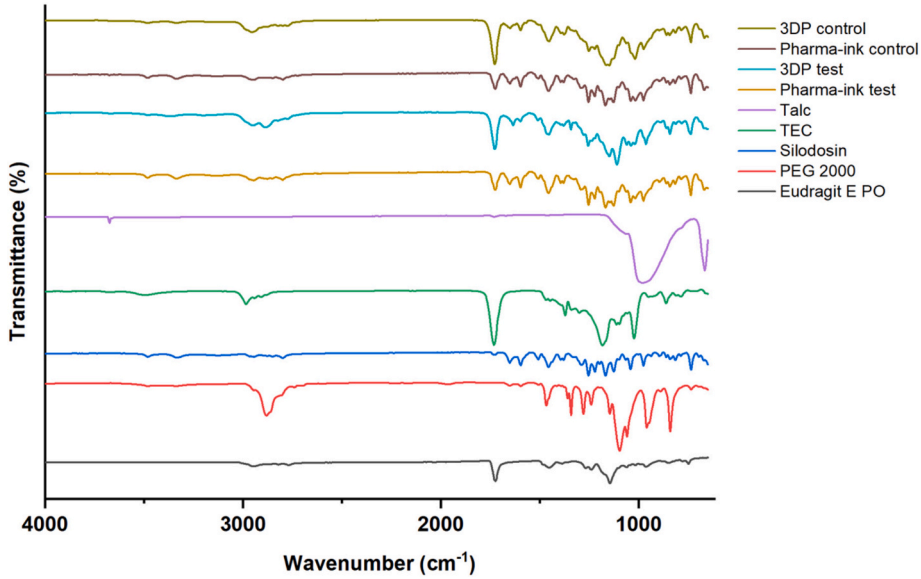

Fig. 7. FT-IR spectra of pure silodosin, excipients, pharma-inks and the printlets.

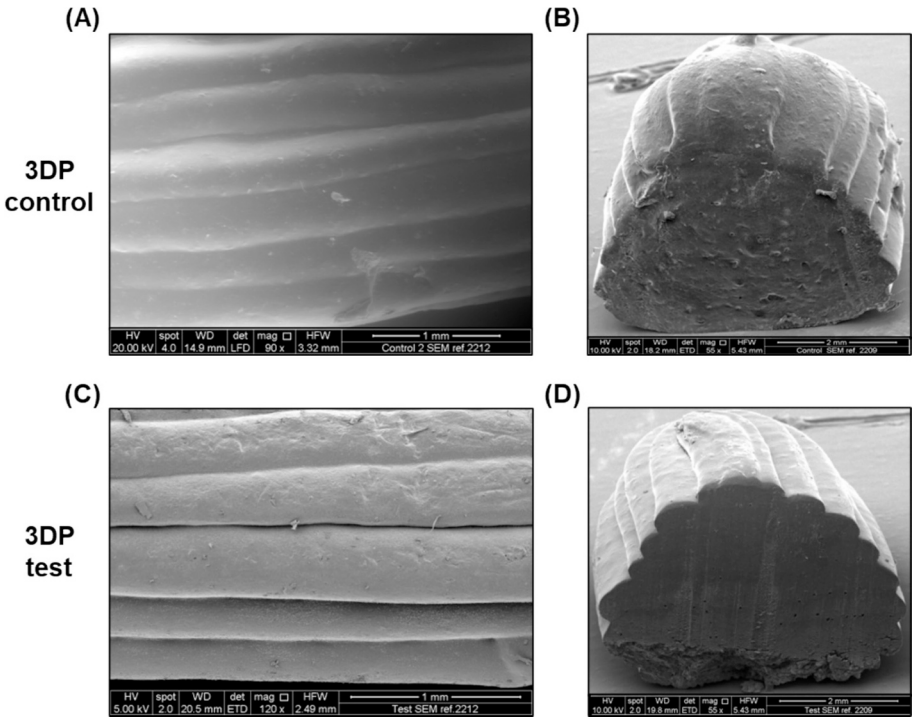

Fig. 8. SEM images of the printlets: (A) layer surface of control; (B) cross-section of control; (C) layer surface of test; (D) cross-section of test. The scale bars for (A) and (C) are 1 mm, and for (B) and (D) are 2 mm.

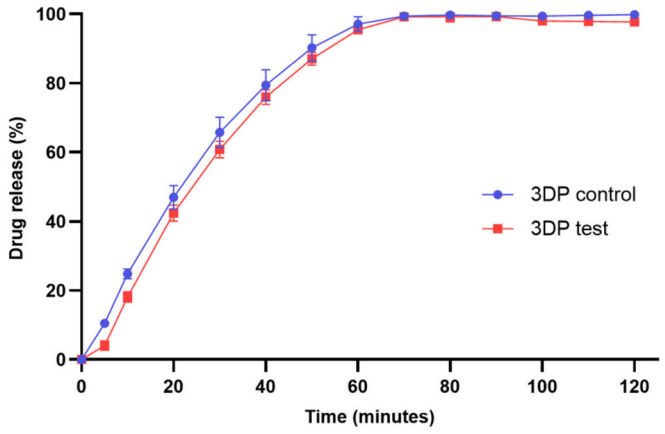

Fig. 9. Dissolution profiles of silodosin from the control and test printlets (n = 3).

the printlets were designed to erode and release silodosin within this window. Complete drug release was achieved by 70 min for both formulations, confirming their suitability for the preclinical study.

Furthermore, the dissolution profiles of the control and test printlets were quantitatively compared using the f_2 similarity factor. The calculated f_2 value was 88.62, which falls within the accepted range of 50–100, indicating a very high similarity between the dissolution profiles. This was essential to minimise variability between the formulations, particularly in dissolution rates, as such differences could potentially alter drug PK. These results also confirm that the absence of PEG 2000 in the control formulation did not adversely impact silodosin release.

3.4. Impact of 3D printing on silodosin pharmacokinetic performance

Figs. 10A and B reveal distinct differences in the mean plasma concentration–time profiles of silodosin between formulation types and sexes. In both male and female rats, control and test solution groups exhibited shorter T_{max} (32–65 min) and higher C_{max} values (4.00–7.11 μg/mL) (Table 5), indicative of rapid drug absorption, with initial peaks followed by a rapid decline in plasma concentration. This can be attributed to the immediate availability of both silodosin and PEG 2000 in the dissolved state following oral administration, leading to a rapid onset of absorption and subsequent swift systemic clearance. However, such rapid absorption may also shorten the duration of PEG 2000 exposure at the intestinal mucosa, particularly as dilution occurs within gastric and intestinal fluids, thereby limiting its interaction with P-gp transporters.

In contrast, printlets (control and test) showed delayed T_{max} in both sexes (140–200 min), suggesting slower and more prolonged drug absorption. The gradual matrix erosion of the solid dosage form appears to have contributed to a steady release of silodosin, thereby extending the absorption window. Notably, in male rats, the 3DP test printlet produced a considerably higher C_{max} of 6.46 μg/mL and a delayed T_{max} of 200 min, accompanied by a substantially increased $AUC_{0-\infty}$ of 1977.03 μg·min/mL compared with the 3DP control (C_{max} 2.60 μg/mL and $AUC_{0-\infty}$ 679.17 μg·min/mL). This is likely due to prolonged mucosal contact of PEG 2000 with P-gp transporters, maintaining local inhibition and enhancing silodosin uptake over time, resulting in a substantially greater increase in overall exposure than the test solution containing the same amount of PEG 2000. The gradual release of PEG 2000 from the solid matrix also reduces luminal dilution, maintaining a higher effective local concentration at the epithelial surface. Since PEGs are highly hydrophilic compounds [47], PEG 2000 is expected to release faster from the printlet matrix than silodosin, facilitating early P-gp modulation and aiding subsequent drug absorption. Conversely, in female rats, the 3DP test group displayed a flatter profile with a lower C_{max} of 3.44 μg/mL at a T_{max} of 160 min and an $AUC_{0-\infty}$ of 1228.42 μg·min/mL. Although this was slightly higher than the 3DP control ($AUC_{0-\infty}$ 882.22 μg·min/mL), the overall curve remained broad and less pronounced, indicating limited influence of PEG 2000 on P-gp activity in females.

Fig. 11 shows the percentage difference in mean $AUC_{0-\infty}$ of silodosin

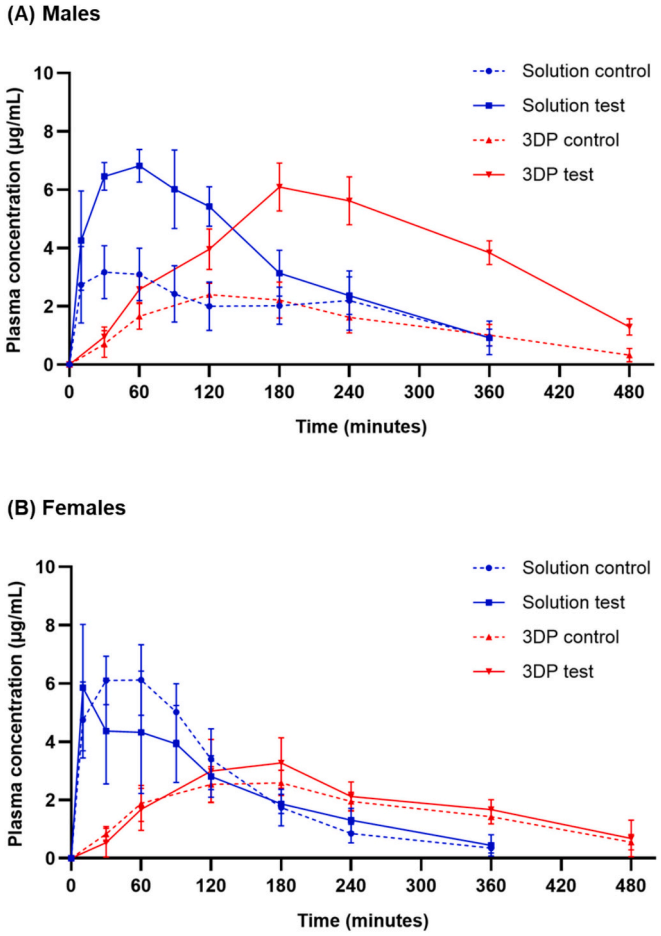

Fig. 10. *In vivo* mean plasma concentration–time profiles of silodosin following oral administration as either solution or 3DP printlet, in the absence or presence of PEG 2000 (1 % *w/v* in solution, equivalent to 5 mg in printlets), in (A) Male and (B) Female rats. Data are expressed as mean ± SD ($n = 6$).

Table 5
Influence of PEG 2000 and formulation strategy on the PK parameters of silodosin in male and female Wistar rats. Data are presented as mean ± SD ($n = 6$).

Formulation	Sex	T_{max} (min)	C_{max} (µg/mL)	AUC_{0-360} /AUC_{0-480} (µg.min/mL)	$AUC_{0-\infty}$ (µg.min/mL)
Solution control	Male	51.67 ± 27.87	4.00 ± 0.75	730.36 ± 114.94	1014.47 ± 164.55
	Female	55.00 ± 22.58	6.57 ± 0.95	894.58 ± 154.71	936.01 ± 156.20
Solution test	Male	65.00 ± 22.58	7.11 ± 0.52	1279.28 ± 99.71	1512.52 ± 259.17
	Female	31.67 ± 34.88	6.63 ± 1.72	804.95 ± 123.20	889.18 ± 131.57
3DP control	Male	140.00 ± 30.98	2.60 ± 0.47	619.26 ± 106.47	679.17 ± 142.65
	Female	150.00 ± 32.86	2.78 ± 0.43	751.14 ± 82.45	882.22 ± 95.10
3DP test	Male	200.00 ± 30.98	6.46 ± 0.62	1766.62 ± 120.13	1977.03 ± 140.34
	Female	160.00 ± 30.98	3.44 ± 0.78	884.81 ± 144.40	1228.42 ± 512.49

normalised to the control between the solution and 3DP formulation groups in male and female Wistar rats. In female rats, no statistically significant differences were observed between the solution and 3DP formulations, with mean percentage differences of −2 % and +42 %, respectively. The slight percentage increase in AUC observed with the

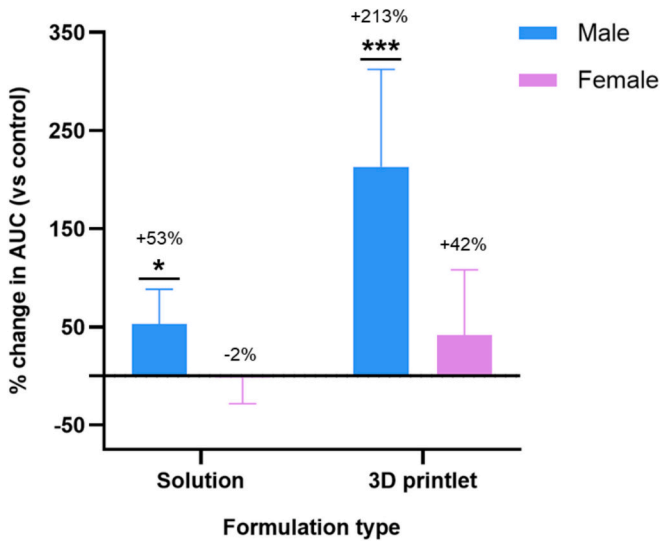

Fig. 11. Percentage change in the mean plasma $AUC_{0-\infty}$ of silodosin in male and female Wistar rats relative to the control. Silodosin was administered either as a solution or 3D printlet, in the absence or presence of PEG 2000 (1 % *w/v* in solution, equivalent to 5 mg in printlets). Data are presented as mean ± SD ($n = 6$). Statistically significant differences are indicated as follows: $p<0.033$ (*), $p<0.002$ (**), $p<0.001$ (***).

3DP printlets may be attributed to the slower erosion of the solid matrix, leading to prolonged drug release and intestinal residence time, but without any significant effect on P-gp modulation. This further supports previous findings that silodosin absorption in females remains largely unaffected by PEG 2000, regardless of its concentration or formulation type.

In male rats, however, striking sex differences were evident. The 1 % *w/v* PEG 2000 solution produced a +53 % increase in AUC in the current study ($n = 6$), which was greater than the +36 % increase observed in the initial solution screening study ($n = 3$). The enhancement was far superior with the 3DP printlets, where silodosin plasma exposure was elevated by +213 % (3.1-fold) compared to the control. This trend is consistent with previously reported human studies, in which co-formulation with PEG 400 increased the oral bioavailability of two P-gp substrate drugs, ranitidine (up to 63 %) and cimetidine (up to 58 %) in male subjects, whereas in female subjects the same formulations produced no enhancement and, in some cases, a reduction in exposure [7,8]. The greater increases observed in the present study suggest that the combination of PEG 2000 and DPE 3DP produced an additive boosting effect on silodosin absorption.

Overall, the amplified PK performance of silodosin observed in male rats is driven by both formulation design and a sex-specific response to PEG 2000. While the inhibition of P-gp activity by PEG-based excipients is well known, this study, to our knowledge, is the first to systematically demonstrate and exploit concentration-dependent and sex-specific effects of PEG 2000 on P-gp-mediated drug absorption *in vivo*, resulting in markedly different PK outcomes between male and female rats. This outcome strongly supports the growing regulatory emphasis on recognising 'sex' as a biological variable and mandating sex-disaggregated data reporting in pharmaceutical research, moving away from the historical "one-size-fits-all" paradigm [58]. This study also highlights that bioequivalence in medicines cannot be reliably extrapolated from males to females, due to the modulatory effects of excipients on biological pathways such as P-gp. The use of Wistar rats, which display sex-dependent intestinal P-gp expression patterns comparable to those in humans, further strengthens the translational relevance of these findings. As such, 3D printing technology is uniquely positioned to enable the personalisation of medicines, allowing the manufacture of sex-specific medicines. Co-formulation with functional excipients such as

PEG 2000 not only improves the oral bioavailability of poorly permeable drugs affected by P-gp efflux but also offers opportunities for dose reduction, decreased API load, and lower overall treatment costs. This approach may be particularly valuable for drugs primarily prescribed to one sex, such as silodosin in male patients. Moreover, the PEG 2000 concentrations used in this study fall within established regulatory safety limits, further supporting the feasibility of clinical translation [59].

4. Conclusion

This study introduces a novel approach to developing sex-specific 3D printed oral medicines by exploiting the pharmacological effects of excipients traditionally viewed as inert, for therapeutic benefit. PEG 2000 was shown to modulate drug absorption in a concentration- and sex-dependent manner. Co-administration of silodosin with 1 % *w/v* PEG 2000 significantly increased systemic drug exposure by 36 % in male Wistar rats compared to the control, with no effect observed in females. When incorporated into silodosin-loaded printlets fabricated *via* DPE 3D printing, PEG 2000 drove a 213 % enhancement in plasma exposure in males but not females. Both formulations exhibited highly similar dissolution profiles ($f_2 = 88.6$) and complete drug release within 70 min, confirming that the PK enhancement was driven by excipient-mediated modulation rather than release kinetics. These findings demonstrate the feasibility of integrating functional, off-the-shelf excipients into 3D printed dosage forms to improve the oral bioavailability of poorly absorbed P-gp substrate drugs. By adjusting excipient concentration, systemic exposure can be optimised in a sex-specific manner, enabling reduced drug doses, lower API loads, and improved formulation sustainability. This study presents excipient-driven 3D printing as an innovative strategy for developing clinically translatable, sex-specific personalised medicines.

CRediT authorship contribution statement

Laxmi Prasanna Nandiraju: Writing – review & editing, Writing – original draft, Visualization, Project administration, Methodology, Investigation, Formal analysis, Data curation, Conceptualization. **Patricija Januskaite:** Writing – review & editing, Visualization, Methodology, Investigation, Formal analysis, Data curation. **Siying Ruan:** Investigation, Formal analysis, Data curation. **Yujia Qin:** Investigation, Formal analysis, Data curation. **Iria Seoane-Viaño:** Writing – review & editing, Methodology, Investigation, Data curation. **Christine M. Madla:** Writing – review & editing, Visualization, Methodology, Data curation, Conceptualization. **Keying Chen:** Investigation, Formal analysis, Data curation. **Alvaro Goyanes:** Writing – review & editing, Supervision, Conceptualization. **Yang Mai:** Writing – review & editing, Visualization, Supervision, Resources, Methodology, Funding acquisition, Formal analysis, Data curation, Conceptualization. **Abdul W. Basit:** Writing – review & editing, Supervision, Resources, Project administration, Funding acquisition, Conceptualization.

Declaration of competing interest

The authors declare no known competing financial interests or personal relationships that could have influenced the work reported in this paper. Alvaro Goyanes and Abdul W. Basit are co-founders of FABRX Ltd. and report relationships with FABRX that include equity or stocks.

Data availability

Data will be made available on request.

Acknowledgements

The authors acknowledge the funding received from the Engineering and Physical Sciences Research Council (EPSRC, UK), [grant numbers EP/S023054/1 and EP/L01646X] to UCL School of Pharmacy, and from the National Natural Science Foundation of China [grant number 82003672]. This work was also supported by the postdoctoral fellowship from Consellería de Cultura, Educación e Universidade (Xunta de Galicia, Spain) [grant number ED481D-2024-011], as well as partial funding from Xunta de Galicia [grant number ED431C 2024/09] and Ministerio de Ciencia, Innovación y Universidades [grant number PID2023-149544OB-C22].

The authors also thank Andrew Weston for assistance with SEM imaging and Haya Alfassam for assistance with FT-IR spectroscopy at the UCL School of Pharmacy. The graphical abstract was created using BioRender.com.

Appendix A. Supplementary data

Supplementary data to this article can be found online at https://doi.org/10.1016/j.jconrel.2025.114577.

References

[1] A. Katdare, M.V. Chaubal, Excipient Development for Pharmaceutical, Biotechnology, and Drug Delivery Systems, Informa Healthcare, 2006.
[2] D. Reker, et al., "Inactive" ingredients in oral medications, Sci. Transl. Med. 11 (483) (2019) eaau6753.
[3] D. Reker, et al., Machine learning uncovers food- and excipient-drug interactions, Cell Rep. 30 (11) (2020) 3710–3716.e4.
[4] T. Flanagan, Potential for pharmaceutical excipients to impact absorption: a mechanistic review for BCS class 1 and 3 drugs, Eur. J. Pharm. Biopharm. 141 (2019) 130–138.
[5] C. Stillhart, et al., Impact of gastrointestinal physiology on drug absorption in special populations—an UNGAP review, Eur. J. Pharm. Sci. 147 (2020) 105280.
[6] M.N. Martinez, et al., A critical overview of the biological effects of excipients (part I): impact on gastrointestinal absorption, AAPS J. 24 (3) (2022).
[7] D.A.I. Ashiru, R. Patel, A.W. Basit, Polyethylene glycol 400 enhances the bioavailability of a BCS class III drug (ranitidine) in male subjects but not females, Pharm. Res. 25 (10) (2008) 2327–2333.
[8] Y. Mai, et al., Boosting drug bioavailability in men but not women through the action of an excipient, Int. J. Pharm. 587 (2020) 119678.
[9] F. Afonso-Pereira, et al., Sex differences in excipient effects: enhancement in ranitidine bioavailability in the presence of polyethylene glycol in male, but not female, rats, Int. J. Pharm. 506 (1) (2016) 237–241.
[10] Y. Mai, et al., Excipient-mediated alteration in drug bioavailability in the rat depends on the sex of the animal, Eur. J. Pharm. Sci. 107 (2017) 249–255.
[11] Y. Mai, et al., Sex-dependence in the effect of pharmaceutical excipients: Polyoxyethylated Solubilising excipients increase Oral drug bioavailability in male but not female rats, Pharmaceutics 11 (5) (2019) 228.
[12] Y. Mai, et al., Quantification of P-glycoprotein in the gastrointestinal tract of humans and rodents: methodology, gut region, sex, and species matter, Mol. Pharm. 18 (5) (2021) 1895–1904.
[13] I. González-Álvarez, et al., Exploring a bioequivalence failure for silodosin products due to Disintegrant excipients, Pharmaceutics 14 (12) (2022).
[14] K.B. Lim, Epidemiology of clinical benign prostatic hyperplasia, Asian J. Urol. 4 (3) (2017) 148–151.
[15] PubChem Compound Summary for CID 5312125, Silodosin, Available from: https://pubchem.ncbi.nlm.nih.gov/compound/Silodosin, 2025.
[16] SILODOSIN capsule, Available from: https://dailymed.nlm.nih.gov/dailymed/drugInfo.cfm?setid=94bca72c-c74a-4181-8b6a-a0a2f654a0a7, 2025.
[17] I. Seoane-Viaño, et al., Translating 3D printed pharmaceuticals: from hype to real-world clinical applications, Adv. Drug Deliv. Rev. 174 (2021) 553–575.
[18] C.J. Parramon-Teixido, et al., A framework for conducting clinical trials involving 3D printing of medicines at the point-of-care, Drug Deliv. Transl. Res. 15 (9) (2025) 3078–3097.
[19] K.G. Mohammed, et al., Pharmaceutical 3D printing in Africa: A scoping review of trends, challenges, and implications for future adoption, Int. J. Pharm. 687 (2026) 126347.
[20] A. Goyanes, et al., Direct powder extrusion 3D printing: fabrication of drug products using a novel single-step process, Int. J. Pharm. 567 (2019) 118471.
[21] Á. Aguilar-de-Leyva, et al., 3D printing direct powder extrusion in the production of drug delivery systems: state of the art and future perspectives, Pharmaceutics 16 (4) (2024) 437.
[22] M. Pistone, et al., Direct cyclodextrin based powder extrusion 3D printing of budesonide loaded mini-tablets for the treatment of eosinophilic colitis in paediatric patients, Int. J. Pharm. 632 (2023) 122592.
[23] H. Wang, et al., Preparation of core-shell controlled release tablets using direct powder extrusion 3D printing techniques, J. Drug Delivery Sci. Technol. 88 (2023) 104896.
[24] I. Seoane-Viaño, et al., A case study on decentralized manufacturing of 3D printed medicines, Int. J. Pharm. X 5 (2023) 100184.

[25] O. Jennotte, et al., Feasibility study of the use of a homemade direct powder extrusion printer to manufacture printed tablets with an immediate release of a BCS II molecule, Int. J. Pharm. 646 (2023) 123506.
[26] G.F. Racaniello, et al., 3D printed mucoadhesive orodispersible films manufactured by direct powder extrusion for personalized clobetasol propionate based paediatric therapies, Int. J. Pharm. 643 (2023) 123214.
[27] M. Pistone, et al., Direct cyclodextrin-based powder extrusion 3D printing for one-step production of the BCS class II model drug niclosamide, Drug Deliv. Transl. Res. 12 (8) (2022) 1895–1910.
[28] J.J. Ong, et al., 3D printed opioid medicines with alcohol-resistant and abuse-deterrent properties, Int. J. Pharm. 579 (2020) 119169.
[29] M. Fanous, et al., Simplification of fused deposition modeling 3D-printing paradigm: feasibility of 1-step direct powder printing for immediate release dosage form production, Int. J. Pharm. 578 (2020) 119124.
[30] M. Rosch, et al., Development of an immediate release excipient composition for 3D printing via direct powder extrusion in a hospital, Int. J. Pharm. 643 (2023) 123218.
[31] G. Mora-Castaño, et al., Optimising 3D printed medications for rare diseases: in-line mass uniformity testing in direct powder extrusion 3D printing, Int. J. Pharm. 668 (2025) 124964.
[32] J. Boniatti, et al., Direct powder extrusion 3D printing of Praziquantel to overcome neglected disease formulation challenges in Paediatric populations, Pharmaceutics 13 (8) (2021) 1114.
[33] P. Januskaite, et al., Sex-specific formulations of doxazosin mesylate via direct powder extrusion 3D printing, Drug Deliv. Transl. Res. 15 (2025) 3338–3350.
[34] A. Alhayali, P.R. Vuddanda, S. Velaga, Silodosin oral films: development, physico-mechanical properties and in vitro dissolution studies in simulated saliva, J. Drug Delivery Sci. Technol. 53 (2019) 101122.
[35] E.L. McConnell, A.W. Basit, S. Murdan, Measurements of rat and mouse gastrointestinal pH, fluid and lymphoid tissue, and implications for in-vivo experiments, J. Pharm. Pharmacol. 60 (1) (2008) 63–70.
[36] M.C. Gohel, et al., Mathematical approach for the assessment of similarity factor using a new scheme for calculating weight, Indian J. Pharm. Sci. 71 (2) (2009) 142–144.
[37] V.P. Shah, et al., In vitro dissolution profile comparison—statistics and analysis of the similarity factor, f2, Pharm. Res. 15 (6) (1998) 889–896.
[38] A.W. Basit, et al., The effect of polyethylene glycol 400 on gastrointestinal transit: implications for the formulation of poorly-water soluble drugs, Pharm. Res. 18 (8) (2001) 1146–1150.
[39] J.D.R. Schulze, et al., Concentration-dependent effects of polyethylene glycol 400 on gastrointestinal transit and drug absorption, Pharm. Res. 20 (12) (2003) 1984–1988.
[40] E.D. Hugger, K.L. Audus, R.T. Borchardt, Effects of poly(ethylene glycol) on efflux transporter activity in Caco-2 cell monolayers, J. Pharm. Sci. 91 (9) (2002) 1980–1990.
[41] Q. Shen, et al., Modulation of intestinal P-glycoprotein function by polyethylene glycols and their derivatives by in vitro transport and in situ absorption studies, Int. J. Pharm. 313 (1–2) (2006) 49–56.
[42] N.N. Salama, et al., Effect of the biologically active fragment of zonula occludens toxin, ΔG, on the intestinal paracellular transport and oral absorption of mannitol, Int. J. Pharm. 251 (1) (2003) 113–121.
[43] P.G. Komarov, et al., Inhibition of cytarabine-induced MDR1 (P-glycoprotein) gene activation in human tumor cells by fatty acid-polyethylene glycol-fatty acid diesters, novel inhibitors of P-glycoprotein function, Int. J. Cancer 68 (2) (1996) 245–250.
[44] H. Yuan, et al., Stearic acid-g-chitosan polymeric micelle for Oral drug delivery: in vitro transport and in vivo absorption, Mol. Pharm. 8 (1) (2011) 225–238.
[45] B. Ucpinar Durmaz, A. Aytac, Effects of polyol-based plasticizer types and concentration on the properties of polyvinyl alcohol and casein blend films, J. Polym. Environ. 29 (1) (2021) 313–322.
[46] R. Kumar, et al., Effect of poly (ethylene glycol) on 3D printed PLA/PEG blend: a study of physical, mechanical characterization and printability assessment, J. Mech. Behav. Biomed. Mater. 141 (2023) 105813.
[47] A.A. D'souza, R. Shegokar, Polyethylene glycol (PEG): a versatile polymer for pharmaceutical applications, Expert Opin. Drug Deliv. 13 (9) (2016) 1257–1275.
[48] S.U. Schilling, et al., Citric acid as a solid-state plasticizer for Eudragit RS PO, J. Pharm. Pharmacol. 59 (11) (2010) 1493–1500.
[49] M. Kuźmińska, et al., Solvent-free temperature-facilitated direct extrusion 3D printing for pharmaceuticals, Int. J. Pharm. 598 (2021) 120305.
[50] L. Liu, et al., Citric acid enhances the activities of Astilbin on psoriasis via Down-regulation of P-glycoprotein, Mol. Pharm. 20 (4) (2023) 1964–1974.
[51] R.I. Moustafine, et al., Eudragit E PO as a complementary material for designing Oral drug delivery systems with controlled release properties: comparative evaluation of new Interpolyelectrolyte complexes with countercharged Eudragit L100 copolymers, Mol. Pharm. 10 (7) (2013) 2630–2641.
[52] Tablet Friability [cited 2025 December 19]; Available from: https://www.usp.org/harmonization-standards/pdg/excipients/tablet-friability, 2023.
[53] R.A. Husseini, et al., Fabrication and optimization of a silodosin in situ-forming PLGA implants for the treatment of benign prostatic hyperplasia: in vitro and in vivo study, Pharmaceutics 16 (11) (2024) 1364.
[54] X. Liu, X. Liu, Y. Hu, Investigation of the thermal decomposition of talc, Clay Clay Miner. 62 (2) (2014) 137–144.
[55] M. Sadia, et al., Channelled tablets: an innovative approach to accelerating drug release from 3D printed tablets, J. Control. Release 269 (2018) 355–363.
[56] C. Tuleu, et al., Gastrointestinal transit of pellets in rats: effect of size and density, Int. J. Pharm. 180 (1) (1999) 123–131.
[57] S.F. Jang, et al., Size discrimination in rat and mouse gastric emptying, Biopharm. Drug Dispos. 34 (2) (2013) 107–124.
[58] C.M. Madla, et al., Let's talk about sex: differences in drug therapy in males and females, Adv. Drug Deliv. Rev. 175 (2021) 113804.
[59] Propylene glycol used as an excipient [cited 2025 October 21]; Available from: https://www.ema.europa.eu/en/documents/report/propylene-glycol-used-excipient-report-published-support-questions-and-answers-propylene-glycol-used-excipient-medicinal-products-human-use_en.pdf, 2017.